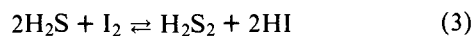


values of $\Delta H^\circ_{558} = 6.19 \pm 0.57$ kcal/mol and $\Delta S^\circ_{558} = 1.6 \pm 1.0$ eu are determined. C_p° of HSI is estimated⁵ by assuming ~ 400 cm⁻¹ as S-I stretching frequency and ~ 1350 cm⁻¹ as deformation frequency of HSI. The contribution from the S-H stretch (2600 cm⁻¹) to C_p° is very small at temperatures considered. Thus, $C_p^\circ_{558(\text{vib})}$ and $C_p^\circ_{298(\text{vib})}$ of HSI are 2.6 ± 0.2 and 1.6 ± 0.2 gibbs/mol, respectively. Adding 8 gibbs/mole for translational and rotational contributions (assuming a nonlinear molecular for HSI), $C_p^\circ_{558} = 10.6 \pm 0.2$ gibbs/mol and $C_p^\circ_{298} = 9.6 \pm 0.2$ gibbs/mol are obtained. $\Delta H^\circ_{298} = 6.28 \pm 0.67$ kcal/mol and $\Delta S^\circ_{298} = 1.8 \pm 1.2$ eu can be obtained by using a value of $\Delta C_p^\circ [= (\Delta C_p^\circ_{298} + \Delta C_p^\circ_{558})/2]$ of -0.3 ± 0.2 gibbs/mol. Combining these with the well-known values of $\Delta H_f^\circ_{298}$ and S°_{298} for I₂, H₂S, and HI⁵ leads to values of $\Delta H_f^\circ_{298}(\text{HSI}, \text{g}) = 10.08 \pm 0.67$ kcal/mol and $S^\circ_{298}(\text{HSI}, \text{g}) = 64.3 \pm 1.2$ eu.

The entropy value of HSI obtained here is in good agreement with the value of $S^\circ_{298} = 64.0 \pm 1.0$ eu estimated from bond additivity.⁵ This lends support to the values obtained. If known values of $\Delta H_f^\circ_{298}(\text{SH}) = 34 \pm 1$ kcal/mol^{5,6} and $\Delta H_f^\circ_{298}(\text{I}) = 25.5$ kcal/mol⁵ are adopted, the bond dissociation energy of HS-I is calculated as 49.4 ± 2 kcal/mol. This is the first quantitative report of a bond strength of a divalent S, RS-I bond.⁶

The secondary reactions are somewhat ambiguous. Plausible secondary products in the system are SI₂, H₂S₂, and HSSI. Reactions for their formation would be



The equilibrium constants for reaction 3 can be calculated from known data⁵ ($\Delta S_{300} = 0$; $\Delta H_{300} = 21.7$ kcal/mol) and shown to lead to negligible H₂S₂ production under the reaction conditions ($K_{(580\text{K})} = 10^{-8.2}$). It is difficult, however, to decide between the remaining two candidate reactions 2 or 4. If SI₂ follows bond additivity then we can estimate $K_2 \approx K_1 \approx 10^{-2}$ and this would account for about 1% further depletion of I₂, which is a factor of 10 from the observed value. A decrease in ΔH_2 from bond additivity of 2.5 kcal, which would be quite plausible,⁷ could account for the secondary reactions.

However, the same type of estimates (somewhat weaker) could be made for reaction 4 so that no definite choice can be made between them from present observations. A choice could be made if we had even crude measurements of the dependence of the fraction of secondary reaction to H₂S pressure. Reaction 4 would be strongly affected by this while reaction 2 would not.

Acknowledgments. This work was supported by the National Science Foundation under Grant CHE-76-16787A01. Helpful discussions with Dr. P. S. Nangia are a pleasure to acknowledge.

References and Notes

- (1) D. M. Golden and S. W. Benson, *Chem. Rev.*, **69**, 125 (1969), and references cited therein.
- (2) H. E. O'Neal and S. W. Benson, "Free Radicals," J. K. Kochi, Ed., Wiley, New York, 1973, Chapter 17.
- (3) (a) E.-C. Wu and A. S. Rodgers, *Int. J. Chem. Kinet.*, **5**, 1001 (1973); (b) *J. Am. Chem. Soc.*, **98**, 6112 (1976); J. M. Pickard and A. S. Rodgers, *ibid.*, **98**, 6115 (1976); **99**, 691, 695 (1977).
- (4) H. Teranishi and S. W. Benson, *J. Am. Chem. Soc.*, **85**, 2890 (1963).
- (5) S. W. Benson, "Thermochemical Kinetics", 2nd ed., Wiley, New York, 1976.
- (6) S. W. Benson, *Chem. Rev.*, **78**, 23 (1978).
- (7) S. W. Benson, *Angew. Chem., Int. Ed. Engl.*, **17**, 812 (1978).

Preparation and Characterization of [*rac*-5,7,7,12,14,14-Hexamethyl-1,4,8,11-tetraazocyclotetradecane]copper(II) *o*-Mercaptobenzoate Hydrate, [Cu(tet b)(*o*-SC₆H₄CO₂)]·H₂O, a Complex with a CuN₄S (Mercaptide) Chromophore

Joseph L. Hughey IV,^{1a} Timothy G. Fawcett,^{1a} Steven M. Rudich,^{1a}
R. A. Lalancette,^{1b} Joseph A. Potenza,^{*1a} and Harvey J. Schugar^{*1a}

Contribution from the Department of Chemistry, Rutgers, The State University of New Jersey, New Brunswick, New Jersey 08903, and the Department of Chemistry, Rutgers, The State University of New Jersey, Newark, New Jersey 07102. Received January 23, 1978

Abstract: The synthesis, crystal structure, electronic spectra, magnetic susceptibility, and ESR data are reported for the title complex. Dark green crystals were obtained in the monoclinic space group $P2_1/n$ with $a = 8.387$ (3) Å, $b = 21.16$ (1) Å, $c = 14.677$ (5) Å, $\beta = 90.92$ (3)°, $d_{\text{obsd}} = 1.32$ (1) g/cm³, $d_{\text{calcd}} = 1.322$ g/cm³, $Z = 4$. Least-squares refinement of 1870 reflections having $F^2 \geq 2\sigma$ gave a conventional R factor of 0.079 and $R_{wF} = 0.095$. The structure consists of Cu(II) monomers with distorted trigonal bipyramidal N₄S ligand donor sets. Structural parameters within the triangular fragment include Cu-S, 2.359 (4) Å; Cu-N, 2.193 (10) and 2.132 (9) Å; S-Cu-N, 120.8 (3) and 135.4 (3)°; and N-Cu-N, 103.5 (4)°. The coordination geometry is completed by two apical Cu-N bonds (2.028 (9), 1.997 (10) Å). Both the X-band ESR spectra ($g_1 = 2.074$, $g_2 = 2.086$ (poorly resolved), $g_3 = 2.117$) and the measured magnetic moment (2.02 (5) μ_B at 293 K) of the polycrystalline complex support its formulation as a Cu(II) N₄S(mercaptide) species. Structural and electronic-spectral data are compared with those reported for analogous CuN₄X (X = Cl, CN) species. The title complex exhibits absorptions at ~ 590 (poorly resolved), 730 ($\epsilon \sim 900$), and ~ 920 nm (shoulder), which are assigned as ligand field transitions. Additional spectral features at 360, 418, and 430 nm which are not exhibited by either free $^-SC_6H_4CO_2^-$ or a reference Zn(tet b)(*o*-SC₆H₄CO₂)·H₂O complex are attributed to S \rightarrow Cu(II) charge transfer.

Introduction

Because of inherent interest in these compounds and their possible usefulness as models for the blue copper proteins, a

number of attempts to prepare Cu^{II}-mercaptide complexes have been reported recently.² However, since nearly all known Cu^{II}-mercaptide systems revert to Cu(I) and disulfide rapidly

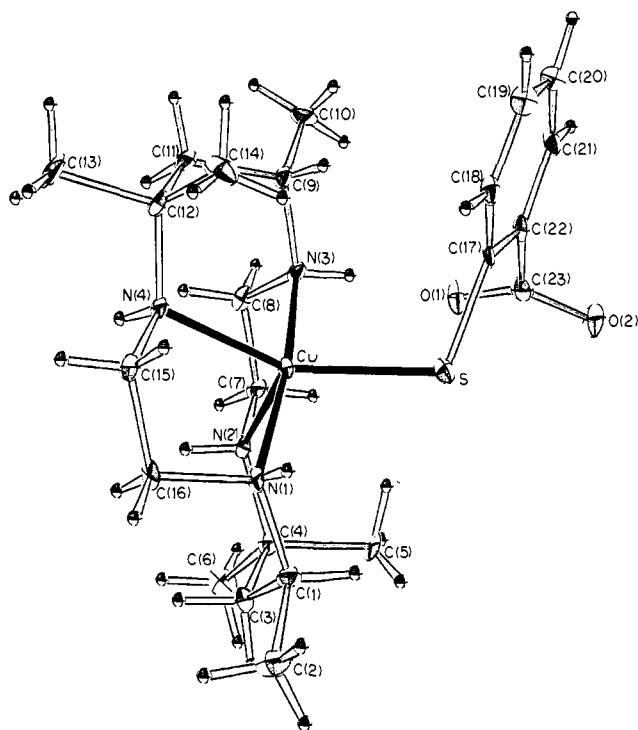


Figure 1. The title complex **1** viewed approximately along the *a* axis and showing the atom numbering scheme. The lattice water molecule has been omitted for clarity.

Table I. Crystal Data for **1**

formula	CuC ₂₃ H ₄₂ N ₄ SO ₃	Z	4
mol wt, g/mol	518.2	<i>d</i> _{obsd} , g/cm ³	1.32 (1), flotation
<i>a</i> , Å	8.387 (3)	<i>d</i> _{calcd} , g/cm ³	1.322
<i>b</i> , Å	21.16 (1)	λ(Mo Kα), Å	0.710 69
<i>c</i> , Å	14.677 (5)	<i>t</i> , °C	25 (1)
β, deg	90.92 (3)	μ, cm ⁻¹	9.8
<i>V</i> , Å ³	2604.4	(Mo Kα)	
space group	<i>P</i> 2 ₁ / <i>n</i>	<i>R</i> _F	0.079
		<i>R</i> _{wF}	0.095

and irreversibly, most studies have been limited to solution species which are transient at room temperature or metastable at low temperatures.

Thus, a metastable, dark blue product obtained from the reaction of Cu(II) and [SP(Ph)₂NP(Ph)₂S]²⁻ at -78 °C has been formulated as a distorted tetrahedral Cu^{II}S₄ species³ while several incompletely characterized, but apparently stable, reaction products of Cu(II) with peptides containing -SH and imidazole groups have been proposed as models for the type 1 copper sites in the blue proteins.⁴ Spectroscopic evidence for the formation of a metastable (~5 min at 10 °C) solution complex of Cu(cyclam)²⁺ (cyclam = 1,4,8,11-tetraazocyclotetradecane) and aliphatic mercaptide ions has been presented.⁵ Extensive ESR, resonance Raman, and electronic-spectral studies have been interpreted in terms of a distorted tetrahedral Cu^{II}N₃S species where tris(pyrazolyl borate) served as the nitrogen donor and either *p*-nitrobenzenethiolate or *O*-ethylcysteinate served as the sulfur donor.⁶ This darkly colored complex was not stable above -30 °C; the corresponding Cu^IN₃S complex was stable, and has been well characterized by an X-ray crystallographic study. Although crystal structures of two Cu^I/Cu^{II}-mercaptide cluster compounds have been reported, their usefulness is hindered by their structural complexities.^{7,8} An approximately tetrahedral CoS₂N₂ chromophore has served to confirm spectral features of Co(II)-substituted derivatives of the copper proteins.⁹

To help understand the nature of Cu^{II}-mercaptide bonding, we have attempted to prepare low molecular weight species stable at room temperature which could be studied conveniently by routine spectroscopic techniques. We report here the synthesis, crystal structure, and preliminary electronic-spectral studies of the title complex (**1**), a stable Cu(II) N₄S(mercaptide) species in which four coordination sites are blocked by the kinetically nonlabile macrocyclic tetramine ligand "tet b".¹⁰ An electronic-spectral reference complex (**2**), formulated as a Zn(II) N₄S(mercaptide) species, has been characterized in part.¹¹

Experimental Section

1. Preparation of the Title Complex (1). Tet b was synthesized by a published procedure,¹² separated from the meso tet a isomer by fractional crystallization, and obtained in pure form as the monohydrate by recrystallization from water-ethanol (mp 98–107 °C, lit.¹³ 97–105 °C). *o*-Mercaptobenzoic acid was obtained from the Aldrich Chemical Co. and recrystallized once from a water-ethanol mixture (mp 165–167 °C, lit.¹⁴ 164 °C). Purple solutions of Cu(tet b)·2ClO₄ were prepared by stirring and gradually warming an alkaline (pH ~ 11) aqueous mixture of the ligand and Cu(H₂O)₆·2ClO₄. Complex **1** was prepared by the reaction in deoxygenated water of Cu(tet b)·2ClO₄ with an excess of *o*-SC₆H₄CO₂⁻·2Na⁺. The dark green, crystalline product is water insoluble and stable "indefinitely" in air when dry. Aqueous suspensions of the product are stable at 95 °C for at least 2 days. In a typical experiment, 1.7 g (65% yield) of product was obtained by reacting 400 mL of a filtered solution 0.012 M in Cu(tet b)²⁺ and 0.05 M in *o*-SC₆H₄CO₂⁻ for 7 days at 55 °C. The product was collected by filtration, washed with water, and dried in air. Infrared absorptions attributable to ClO₄⁻, -SH, and -CO₂H could not be detected in the product; the strong characteristic absorptions of carboxylate were present. A second batch of the above solution was filtered through a Millipore membrane (0.22-μm pore size) and maintained under a N₂ atmosphere at 25 °C for 3 weeks. During this period, relatively well-formed crystals of **1** grew.

Anal. Calcd for CuC₂₃H₄₂N₄SO₃: Cu, 12.26; C, 53.51; H, 8.17; N, 10.81; S, 6.19. Found: Cu, 12.01; C, 53.14; H, 8.67; N, 10.71; S, 6.28.

2. Preparation of Zn(tet b(*o*-SC₆H₄CO₂))·H₂O (2). A solution of 0.60 g (2 mmol) of tet b·H₂O, 4 mL of 1 M HCl, and 0.27 g (2 mmol) of ZnCl₂ was boiled for 10 min, brought to pH ~ 10 with 1 M KOH, and boiled for an additional 10 min. The cooled (25 °C) and deoxygenated solution was mixed under N₂ with 80 mL of a separate solution containing 8 mmol of *o*-SC₆H₄CO₂⁻ (prepared from 1.24 g (8 mmol) of *o*-mercaptobenzoic acid and 16 mL of 1.0 M KOH). After a reaction time of 1 h at 30 °C, the solution deposited 0.73 g (71%) of an off-white solid which was collected by filtration, washed with water, and dried in air. Infrared absorptions attributable to ClO₄⁻, -SH and -CO₂H could not be detected in the product.

Anal. Calcd for ZnC₂₃H₄₂N₄SO₃: C, 53.12; H, 8.14; N, 10.77. Found: C, 52.94; H, 7.93; N, 10.67.

3. Physical Measurements. Infrared spectra were recorded using a Perkin-Elmer Model 225 spectrophotometer. Samples were dispersed as KBr pellets and as mineral oil mulls. Electronic spectra were recorded using a Cary Model 14 spectrophotometer. Samples were dispersed as KBr pellets and as mineral oil mulls; spectra were also recorded of **1** and **2** dissolved in 0.01 M methanolic KOH.

Magnetic susceptibility data for **1** at room temperature were obtained using a Gouy balance calibrated with Ni(en)₃·S₂O₃. ESR spectra of powdered **1** were measured at 298 and 77 K using a Varian Model E-12 spectrometer calibrated with a Hewlett-Packard Model 5245L frequency counter and a DPPH crystal (*g* = 2.0036).

4. Collection of Diffraction Data. Examination of about 12 crystals by film techniques revealed that apparently well-formed crystals of **1** really were aggregates. Repeated cleavage of a large aggregate approximately perpendicular to the *b* direction eventually gave a single crystal of **1** which exhibited slightly asymmetric diffraction peak profiles. This fragment had dimensions of 0.10 × 0.08 × 0.05 mm and was mounted on a glass fiber parallel to the *b* direction. Unit cell parameters (Table I) were determined by a least-squares analysis of the θ , χ , and ϕ values of 15 reflections using graphite-monochromated Mo K α radiation and a Syntex P₂₁ computer-controlled diffractometer. Diffractometer examination of the reciprocal lattice indicated a monoclinic system and space group *P*2₁/*n* (a nonstandard form of

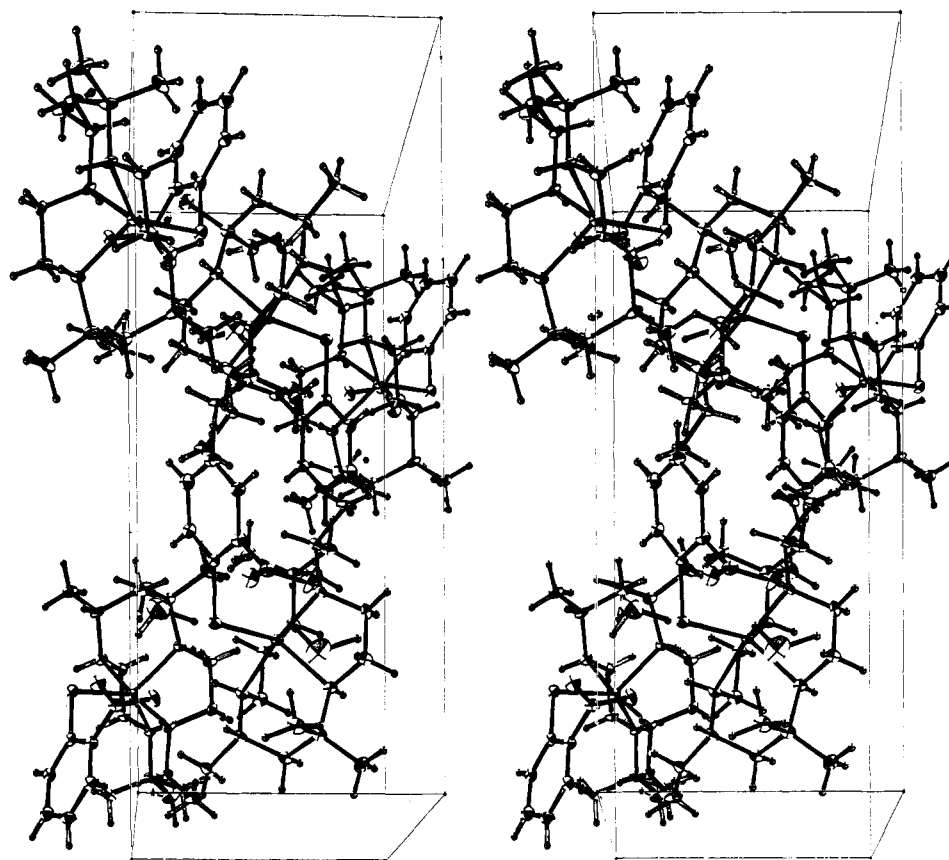


Figure 2. Stereoscopic packing diagram for **1** viewed approximately along *b*. The *a* axis is horizontal.

*P*2₁/*c* with systematic absences $0k0$, $k = 2n + 1$, and $h0l$, $h + l = 2n + 1$. A density of 1.322 g/cm³ was calculated for four molecules of **1** per unit cell and is in good agreement with the value of 1.32 (1) g/cm³ measured by flotation in a mixture of CCl₄ and cyclohexane. A θ - 2θ scan over the range $2^\circ \leq \theta \leq 45^\circ$ was used to collect a total of 4794 reflections. Of these, 1870 having $F^2 \geq 2\sigma(F^2)$ were used in the solution and refinement of the structure. To improve the counting statistics obtained from the relatively small cleaved crystal, a scan rate of $1^\circ/\text{min}$ was employed. Each scan covered a range from 0.7° below the calculated $K\alpha_1$ position to 0.9° above the calculated $K\alpha_2$ position. Stationary background counts were taken before and after each scan. The total time for background counts equaled the scan time and was equally distributed before and after the peak.

The intensities of three standard reflections were recorded every 50 reflections throughout the data collection period; they showed random variations of $\pm 6\%$, but no significant trend. Intensities were calculated from the relationship

$$I = (P - LB - RB)SR$$

where *P* is the peak count, LB is the low-angle background count, RB is the high-angle background count, and SR is the scan rate. These intensities were corrected for any decay by computing average decay factors on the basis of the three standard reflections; 182 peaks were rejected on the basis of a profile scan. The polarization correction for the parallel-parallel mode of the P2₁ diffractometer was chosen assuming the monochromator crystal to be 50% perfect and 50% mosaic.

Initial standard deviations were calculated by

$$\sigma(I) = (P + LB + RB)^{1/2}SR$$

$$\sigma(F_o^2) = (1/Lp)(\sigma^2(I) + (0.03I)^2)^{1/2}$$

Lorentz and polarization factors as well as absorption corrections were applied to all 4794 reflections. The linear absorption coefficient μ for Mo $K\alpha$ radiation was 9.8 cm^{-1} ; maximum and minimum absorption factors for the data collected were 1.16 and 1.11, respectively.

5. Solution and Refinement of the Structure.¹⁵ The structure was solved by direct methods and refined by full-matrix least-squares

techniques. An *E* map, calculated using 280 phases from the starting set having the highest combined figure of merit, revealed the Cu atom and all nonhydrogen atoms of the mercaptide ligand. A difference Fourier map, based on phases determined from these coordinates, revealed all nonhydrogen atoms of the tet b ligand except for three C atoms which were located on a subsequent difference Fourier map. With all nonhydrogen scattering matter present, the initial agreement factor $R_F = \sum ||F_o| - |F_c|| / \sum |F_o|$ was 0.363.

Refinement, based on *F*, was initiated using neutral atom scattering factors^{16a} for all species; both real and imaginary parts of the anomalous dispersion corrections were applied to Cu and S.^{16b} Several cycles of isotropic, followed by anisotropic, refinement reduced *R_F* and $R_{wF} = (\sum w(|F_o| - |F_c|)^2 / \sum w F_o^2)^{1/2}$ to 0.098 and 0.108, respectively. At this point, a difference Fourier map was calculated and H atoms were added to the model. Amine and methylene H coordinates were calculated assuming tetrahedral geometry and N-H and C-H distances¹⁷ of 0.87 and 0.95 Å, respectively. Methyl group H atoms were located by placing tetrahedrally oriented H atoms 0.95 Å from the appropriate C atom; these were rotated at 5° intervals to yield a best fit between the calculated positions and positive regions of electron density on the difference map. Analysis of the difference map revealed several peaks of high electron density approximately 1 Å from the H₂O O atom. One peak, much larger than the others, and in a good position for hydrogen bonding, was assumed to be a H atom. A second peak, which gave an H-O-H angle of 110° and was located 1.1 Å from the O atom, was taken as the second H atom. All H atoms were located in positive regions on the difference Fourier map. Temperature factors for the H atoms were set according to $B_H = B_N + 1$, where N is the atom to which H is bonded. Hydrogen-atom parameters were not refined.

For the final refinement cycles, those incorporating H atoms, a weighting scheme was chosen by an analysis of variance to make $|\Delta F|/\sigma(F_o)$ independent of $|F_o|$. This led to the following assignments for $\sigma(F_o)$:

$$\sigma(F_o) = 2.982 - 0.133|F_o|, \quad |F_o| < 13.78$$

$$\sigma(F_o) = 0.532 + 0.045|F_o|, \quad 13.78 \leq |F_o| \leq 21.63$$

$$\sigma(F_o) = 0.935 + 0.026|F_o|, \quad |F_o| > 21.63$$

Table II. Fractional Atomic Coordinates^a and Thermal Parameters^b for I

atom	x	y	z	β_{11} or $B, \text{\AA}^2$	β_{22}	β_{33}	β_{12}	β_{13}	β_{23}
Cu	3.6 (2)	2435 (1)	-845 (1)	15.9 (3)	17.4 (4)	17.0 (6)	5 (1)	-8.2 (9)	-2.6 (4)
S	-223.2 (4)	2352 (2)	-1810 (2)	16.7 (7)	22 (1)	38 (2)	7 (2)	-20 (3)	-10 (1)
N(1)	-109 (1)	3071 (5)	-47 (6)	15 (2)	21 (3)	15 (4)	3 (6)	-1 (7)	-1 (3)
N(2)	189 (1)	3141 (5)	-1104 (6)	17 (2)	19 (3)	18 (5)	-3 (6)	-2 (8)	2 (3)
N(3)	146 (1)	1851 (5)	-1522 (6)	18 (2)	18 (3)	18 (4)	16 (6)	-9 (8)	-3 (3)
N(4)	77 (1)	2023 (5)	419 (6)	16 (2)	21 (3)	16 (4)	3 (6)	-8 (8)	-1 (3)
O(1)	77 (1)	2053 (5)	-3434 (6)	17 (2)	43 (3)	43 (5)	-23 (7)	-22 (8)	9 (3)
O(2)	-128 (1)	2134 (5)	-4370 (6)	25 (2)	42 (3)	27 (4)	-3 (7)	-27 (8)	10 (3)
O(3)	92 (2)	3134 (7)	-4776 (10)	37 (4)	63 (6)	110 (11)	-38 (12)	-36 (16)	20 (6)
C(1)	-126 (2)	3727 (6)	-444 (8)	20 (3)	22 (4)	31 (7)	19 (9)	-6 (11)	-2 (4)
C(2)	-231 (2)	4137 (7)	166 (12)	30 (4)	25 (4)	74 (10)	27 (11)	54 (17)	0 (5)
C(3)	35 (2)	4039 (6)	-599 (8)	22 (3)	21 (4)	20 (6)	7 (9)	2 (11)	1 (3)
C(4)	142 (2)	3800 (6)	-1341 (8)	19 (3)	21 (4)	27 (7)	2 (8)	12 (11)	7 (4)
C(5)	52 (2)	3805 (7)	-2277 (8)	25 (4)	37 (5)	20 (6)	29 (10)	-7 (11)	9 (4)
C(6)	289 (2)	4231 (7)	-1374 (10)	28 (4)	30 (4)	44 (8)	-17 (11)	37 (14)	4 (5)
C(7)	296 (2)	2812 (6)	-1736 (8)	22 (3)	22 (4)	28 (6)	2 (8)	12 (11)	6 (4)
C(8)	307 (2)	2130 (6)	-1515 (9)	11 (3)	25 (4)	40 (7)	5 (8)	1 (10)	-1 (4)
C(9)	138 (2)	1172 (6)	-1246 (8)	20 (3)	18 (3)	32 (7)	15 (8)	-24 (12)	-3 (4)
C(10)	229 (2)	749 (7)	-1886 (10)	34 (4)	21 (4)	45 (8)	12 (10)	-20 (15)	-3 (4)
C(11)	191 (2)	1066 (6)	-236 (9)	25 (3)	19 (3)	43 (7)	8 (9)	-31 (13)	6 (4)
C(12)	83 (2)	1318 (6)	510 (8)	27 (4)	20 (4)	27 (6)	1 (9)	-6 (12)	6 (4)
C(13)	163 (2)	1133 (8)	1433 (10)	41 (5)	38 (5)	33 (7)	48 (13)	-28 (16)	10 (5)
C(14)	-82 (2)	1044 (7)	435 (10)	25 (4)	26 (4)	58 (9)	-34 (10)	21 (14)	-2 (5)
C(15)	-17 (2)	2344 (6)	1124 (7)	21 (3)	27 (4)	13 (5)	-2 (8)	-1 (9)	3 (3)
C(16)	-37 (2)	3036 (6)	879 (8)	23 (3)	26 (4)	16 (5)	-1 (9)	-2 (11)	-2 (4)
C(17)	-227 (2)	1575 (6)	-2296 (8)	13 (2)	24 (4)	27 (6)	4 (7)	-27 (10)	-9 (4)
C(18)	-311 (2)	1092 (7)	-1852 (8)	18 (3)	29 (4)	24 (6)	-14 (9)	-6 (10)	0 (4)
C(19)	-316 (2)	490 (7)	-2181 (10)	23 (3)	27 (5)	51 (9)	-8 (10)	-7 (14)	2 (5)
C(20)	-236 (2)	348 (7)	-2983 (11)	29 (4)	19 (4)	61 (10)	0 (10)	-28 (16)	-6 (5)
C(21)	-157 (2)	815 (7)	-3445 (9)	21 (3)	28 (4)	32 (7)	-3 (9)	-30 (12)	-9 (5)
C(22)	-151 (2)	1428 (6)	-3110 (8)	16 (3)	22 (3)	24 (6)	-1 (7)	-25 (10)	-2 (4)
C(23)	-61 (2)	1915 (6)	-3656 (8)	17 (3)	25 (4)	32 (7)	-4 (9)	-12 (11)	-2 (4)
H(N1)	-209	293	0	3.4					
H(N2)	241	316	-60	3.4					
H(N3)	115	187	-210	3.4					
H(N4)	178	216	53	3.3					
H1(C1)	-177	370	-103	4.3					
H1(C2)	-179	422	72	5.7					
H2(C2)	-256	453	-14	5.7					
H3(C2)	-329	392	27	5.7					
H1(C3)	95	406	-3	4.3					
H2(C3)	22	449	-67	4.3					
H1(C5)	30	336	-234	5.1					
H2(C5)	-54	396	-220	5.1					
H3(C5)	125	386	-276	5.1					
H1(C6)	348	421	-80	5.6					
H2(C6)	362	408	-184	5.6					
H3(C6)	262	465	-150	5.6					
H1(C7)	402	300	-167	3.6					
H2(C7)	262	286	-235	3.6					
H1(C8)	354	208	-92	4.4					
H2(C8)	373	192	-194	4.4					
H(C9)	26	104	-128	4.4					
H1(C10)	136	50	-185	5.3					

atom	x	y	z	β_{11} or $B, \text{\AA}$
H2(C10)	237	93	-247	5.3
H3(C10)	314	53	-155	5.3
H1(C11)	215	62	-14	4.1
H2(C11)	298	125	-16	4.1
H1(C13)	96	124	193	5.6
H2(C13)	183	68	146	5.6
H3(C13)	263	135	152	5.6
H1(C14)	-77	59	40	5.7
H2(C14)	-142	115	97	5.7
H3(C14)	-137	120	-9	5.7
H1(C15)	-122	215	113	4.1
H2(C15)	30	230	171	4.1
H1(C16)	-107	324	131	3.7
H2(C16)	65	323	88	3.7
H(C18)	-361	119	-129	4.5
H(C19)	-377	17	-187	5.3
H(C20)	-237	-8	-322	5.2
H(C21)	-105	71	-400	4.5
H1(O3)	220	297	-476	9.9
H2(O3)	20	281	-455	9.9

^a Hydrogen atoms and all x coordinates are $\times 10^3$; the remaining coordinates are $\times 10^4$. ^b Values for β_{11} are $\times 10^3$; the remaining anisotropic temperature factors are $\times 10^4$. The form of the thermal ellipsoid is $\exp[-(\beta_{11}h^2 + \beta_{22}k^2 + \beta_{33}l^2 + 2\beta_{12}hk + 2\beta_{13}hl + 2\beta_{23}kl)]$.

Several cycles of anisotropic refinement led to convergence with $R_F = 0.079$ and $R_{wF} = 0.095$. For the final cycle, all parameter changes were within their estimated standard deviation. A final difference map showed two residuals ($0.8 \text{ e}/\text{\AA}^3$) in the vicinity of the Cu atom which were somewhat larger than the general background ($\pm 0.5 \text{ e}/\text{\AA}^3$). Final atomic parameters are listed in Table II while views of the title complex (showing the atom numbering scheme) and its packing are given in Figures 1 and 2, respectively. A list of observed and calculated structure factors is available.¹⁸

Results and Discussion

Description of the Structure. The structure consists of discrete Cu(II) monomers with approximately trigonal bipyramidal N_4S ligand donor sets. Bond angles (Table III) within

the equatorial $\text{CuSN}(2)\text{N}(4)$ fragment follow: S-Cu-N(2), $120.8 (3)^\circ$; S-Cu-N(4), $135.4 (3)^\circ$; N(2)-Cu-N(4), $103.5 (4)^\circ$. The apical N(3)-Cu-N(1) fragment is bent ($170.8 (4)^\circ$) while the six bond angles involving the equatorial CuSN_2 fragment and the two apical nitrogen atoms span the range $84.3 (4)$ - $98.0 (3)^\circ$. The observed Cu-S distance (Table III) of $2.359 (4) \text{ \AA}$ is appropriate for a full equatorial bonding interaction. Comparable distances have been reported for Cu^{II} -mercaptide bonding ($\sim 2.28 \text{ \AA}$)^{7,8} and Cu^{II} -thioether bonding (2.366 \AA)¹⁹ within planar CuN_2S_2 units. Evidence for the substantial strength of the Cu-S bond also is implied by the pronounced lengthening of both equatorial Cu-N bonds ($2.193 (10)$, $2.132 (9) \text{ \AA}$) relative to those reported (2.02 - 2.07

Table III. Bond Distances (Å) and Angles (deg) in 1

Distances			
Cu-S	2.359 (4)		
Cu-N(1)	2.028 (9)	N(1)-C(1)	1.51 (2)
Cu-N(2)	2.193 (10)	C(1)-C(2)	1.54 (2)
Cu-N(3)	1.997 (10)	C(1)-C(3)	1.52 (2)
Cu-N(4)	2.132 (9)	C(3)-C(4)	1.51 (2)
Cu...O(1)	3.944 (10)	C(4)-C(5)	1.56 (2)
		C(4)-C(6)	1.53 (2)
		C(4)-N(2)	1.49 (2)
S-C(17)	1.79 (1)	N(2)-C(7)	1.48 (2)
C(17)-C(18)	1.41 (2)	C(7)-C(8)	1.48 (2)
C(18)-C(19)	1.36 (2)	C(8)-N(3)	1.47 (2)
C(19)-C(20)	1.40 (2)	N(3)-C(9)	1.49 (2)
C(20)-C(21)	1.37 (2)	C(9)-C(10)	1.51 (2)
C(21)-C(22)	1.39 (2)	C(9)-C(11)	1.56 (2)
C(22)-C(17)	1.40 (2)	C(11)-C(12)	1.53 (2)
C(22)-C(23)	1.51 (2)	C(12)-C(13)	1.55 (2)
C(23)-O(1)	1.24 (2)	C(12)-C(14)	1.50 (2)
C(23)-O(2)	1.27 (1)	C(12)-N(4)	1.50 (2)
O(1)...O(2)	2.19 (1)	N(4)-C(15)	1.48 (2)
O(1)...O(3)	3.02 (2)	C(15)-C(16)	1.52 (2)
O(2)...O(3)	2.88 (2)	C(16)-N(1)	1.48 (1)
Angles			
N(1)-Cu-N(2)	89.2 (4)	N(1)-Ni-N(2)	(91.2 (4)) ^a
N(1)-Cu-N(3)	170.8 (4)	N(1)-Ni-N(3)	(175.2 (4))
N(1)-Cu-N(4)	84.3 (4)	N(1)-Ni-N(4)	(85.4 (4))
N(2)-Cu-N(3)	84.4 (4)	N(2)-Ni-N(3)	(85.3 (4))
N(2)-Cu-N(4)	103.5 (4)	N(2)-Ni-N(4)	(103.3 (4))
N(3)-Cu-N(4)	90.7 (4)	N(3)-Ni-N(4)	(92.1 (4))
S-Cu-N(1)	90.9 (3)	Cu-N(1)-C(1)	115.3 (7)
S-Cu-N(2)	120.8 (3)	Cu-N(1)-C(16)	108.0 (7)
S-Cu-N(3)	98.0 (3)	Cu-N(2)-C(4)	119.6 (8)
S-Cu-N(4)	135.4 (3)	Cu-N(2)-C(7)	103.1 (7)
		Cu-S-C(17)	108.4 (4)
N(1)-C(1)-C(2)	110.0 (10)		
N(1)-C(1)-C(3)	112.5 (11)	Cu-N(3)-C(9)	115.4 (8)
C(1)-C(3)-C(4)	120.0 (11)	Cu-N(3)-C(8)	107.7 (7)
C(2)-C(1)-C(3)	111.3 (12)	Cu-N(4)-C(12)	119.5 (7)
C(3)-C(4)-C(5)	110.4 (12)	Cu-N(4)-C(15)	105.7 (7)
C(3)-C(4)-C(6)	108.1 (11)		
C(3)-C(4)-N(2)	107.7 (9)	N(3)-C(9)-C(10)	112.0 (11)
C(4)-N(2)-C(7)	117.2 (9)	N(3)-C(9)-C(11)	112.6 (10)
N(2)-C(7)-C(8)	110.9 (11)		
C(7)-C(8)-N(3)	109.7 (12)	C(9)-C(11)-C(12)	118.2 (12)
C(8)-N(3)-C(9)	115.5 (10)	C(10)-C(9)-C(11)	111.6 (11)
		C(11)-C(12)-C(13)	106.5 (13)
S-C(17)-C(22)	122.8 (10)	C(11)-C(12)-C(14)	111.5 (12)
S-C(17)-C(18)	119.1 (10)	C(11)-C(12)-N(4)	107.6 (10)
C(17)-C(18)-C(19)	121.9 (13)	C(12)-N(4)-C(15)	114.2 (9)
C(18)-C(19)-C(20)	119.2 (14)	N(4)-C(15)-C(16)	109.6 (9)
C(19)-C(20)-C(21)	120.1 (13)	C(15)-C(16)-N(1)	108.0 (9)
C(20)-C(21)-C(22)	120.8 (13)	C(16)-N(1)-C(1)	115.6 (9)
C(21)-C(22)-C(17)	119.8 (13)		
C(22)-C(17)-C(18)	118.1 (11)	C(22)-C(23)-O(1)	119.8 (12)
C(21)-C(22)-C(23)	117.6 (12)	C(22)-C(23)-O(2)	117.9 (13)
C(17)-C(22)-C(23)	122.5 (11)	O(1)-C(23)-O(2)	122.1 (13)

^a Values included in parentheses are the corresponding angles reported for the [Ni(tet b)acetate]ClO₄ complex.²²

Å) for structurally analogous CuN₄X (X = Cl,²⁰ CN²¹) coordination geometries. A detailed analysis of the configurational isomers possible for coordinated racemic tet b has been presented by other authors.²² Inspection of Figure 1 reveals that both six-membered chelate rings have the chair conformation, both five-membered chelate rings have the gauche

conformation, and the macrocyclic ligand is folded about the N(3)-Cu-N(1) axis. This folded configuration has the lowest predicted configurational energy of the possible tet b isomers.²² The same tet b conformation was observed by other workers for a dimeric [Cu(tet b)₂Cl³⁺] complex having equivalent N₄Cl ligand donor sets²⁰ and a [Ni(tet b)acetate]ClO₄ complex having a *cis*-N₄O₂ donor set (the acetate is bidentate).²² Even though this latter chromophore is approximately octahedral, the structural parameters of its tet b component closely resemble those reported for the title complex. A comparison (Table III) of corresponding N-metal-N bond angles obtained for the title complex with those reported for the above Ni(II) complex shows that the geometries of the metal-(folded) tet b units nearly are identical for both structures.

Other structural features are revealed by the least-squares planes listed in Table IV. The copper atom is situated only 0.065 and 0.032 Å from the planes defined by N(1), N(3), N(4) and S, N(2), N(4), respectively. The chair conformations of both six-membered chelate rings are characterized additionally by the observed atom deviations from planes II and III. Finally, plane I indicates the substantial and opposite deviations of the sulfur atom and carboxylate carbon atom (C(23)) from the essentially planar aromatic ring. This structural feature is suggestive of steric crowding, and has been observed in crystallographic studies of benzoic acids having bulky ortho substituents such as -Cl²³ and -SO₃⁻.²⁴ An inspection of Figure 1 reveals that the carboxylate group and benzene ring nearly are perpendicular; the actual dihedral angle between the planes defined by the O(1), C(23), O(2) and C(17), C(22), C(21) fragments is 79.0°. For comparison, corresponding rotations of 13.7 and 50.7° have been reported for benzoic acids substituted in the ortho position by -Cl²³ and -SO₃⁻,²⁴ respectively. Hydrogen-bonding interactions (Table V), particularly the intramolecular one between H(N3) and O(1), also serve to twist the carboxylate group. Thus, the unexpectedly large carboxylate group rotation observed for **1** reasonably results from a combination of steric effects and both intra- and intermolecular hydrogen-bonding interactions. Figure 2 portrays these hydrogen-bonding interactions. Neither the carboxylate oxygen atoms nor the water molecule are bound to copper. The closest Cu...O separation in the structure is the Cu...O(1) distance of 3.994 (10) Å.

Electronic Structural Aspects of 1. Our characterization of **1** as a complex of Cu(II) is supported by the observed structural similarities to related Cu^{II}-macrocyclic amine complexes (vide supra), and by magnetic susceptibility, ESR, and electronic-spectral studies. The corrected magnetic moment²⁵ of polycrystalline **1** at 293 K is 2.02 (5) μ_B, and falls within the range observed for magnetically dilute five-coordinate Cu(II) complexes.²⁶ X-Band ESR spectra (not shown) of polycrystalline **1** at 77 K consist of closely spaced signals at g₁ = 2.074, g₂ = 2.086 (poorly resolved), and g₃ = 2.117. Better resolved spectra having comparable g values have been obtained elsewhere at Q-band.²⁷ The observed ESR spectra are appropriate for a magnetically dilute Cu(II) chromophore having rhombic symmetry.

The low-temperature (~90 K) spectra of **1** dispersed in a KBr pellet are presented in Figure 3; a similar band pattern was observed at lower resolution for methanolic KOH solutions (Figure 4), KBr pellets, and mineral oil mulls containing **1** at room temperature. The ε values of the pellet spectra²⁸ are about twice as large as those obtained from solution studies. Comparison of Figures 3 and 4 with the data reported for related CuN₄X (X = Cl, CN) chromophores²¹ indicates that the spectral features at ~920, ~730, and ~590 nm (inferred by asymmetry of the 730-nm band) arise from ligand field absorptions. Comparably intense LF absorptions recently have been reported for other low-symmetry five-coordinate Cu(II) chromophores.²⁶ Additional spectral features at ~430, 418,

Table IV. Least-Squares Planes

plane	atoms defining plane	equation of mean plane ^a
I	C(17)-C(18)-C(19)-C(20)-C(21)-C(22)	$0.3357X_0 - 0.5828Y_0 + 0.7401Z_0 = -4.110$
II	N(4)-C(12)-C(9)-N(3)	$0.8601X_0 + 0.0830Y_0 + 0.5033Z_0 = 1.061$
III	N(1)-C(1)-C(4)-N(2)	$0.3173X_0 + 0.3937Y_0 + 0.8627Z_0 = 0.772$
IV	N(1)-N(3)-N(4)	$0.5692X_0 + 0.7111Y_0 + 0.4127Z_0 = 1.461$
V	S-N(2)-N(4)	$0.1657X_0 + 0.6992Y_0 + 0.6955Z_0 = 1.177$

plane I		Displacement of Atoms from Mean Plane, Å		plane II		plane III		plane IV		plane V	
C(17)	0.011	S	0.033	N(4)	-0.012	N(1)	0.007	N(1)	0.000	S	0.000
C(18)	-0.004	C(23)	-0.025	C(12)	0.014	C(1)	-0.008	N(3)	0.000	N(2)	0.000
C(19)	-0.007	O(1)	1.049	C(9)	-0.015	C(4)	0.008	N(4)	0.000	N(4)	0.000
C(20)	0.013	O(2)	-1.142	N(3)	0.013	N(2)	-0.007	Cu	-0.065	Cu	-0.032
C(21)	-0.006			Cu	-1.132	Cu	-0.422				
C(22)	-0.006			C(11)	0.858	C(3)	0.289				

^a Equations have the form $AX_0 + BY_0 + CZ_0 = D$ where X_0, Y_0, Z_0 are Cartesian axes lying along bxc^* , b , and c^* , respectively.

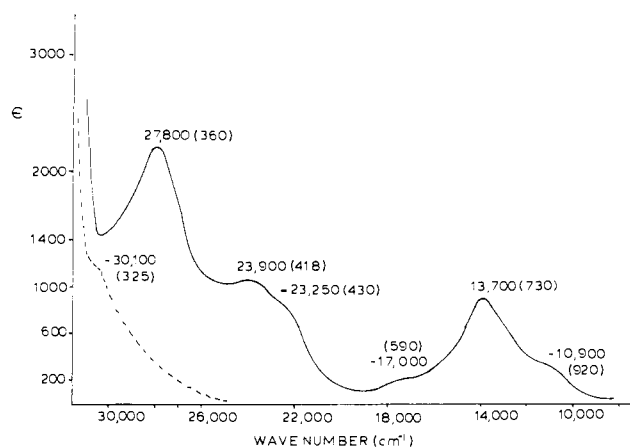


Figure 3. Electronic spectra at ~ 90 K of a "0.04 M solution" of **1** in a 0.0173-cm thick KBr pellet²⁸ (—), and of a "0.026 M solution" of **2** in a 0.020-cm thick KBr pellet(- - -). Peak positions in nanometers are given in parentheses.

and 360 nm are obscured in part by tailing of an intense UV absorption whose λ_{\max} (not shown) is 265 nm. Although uncomplexed $o\text{-HSC}_6\text{H}_4\text{CO}_2^-$ exhibits an absorption band at ~ 350 nm (ϵ 400), the free dianion has only weak end absorption in this spectral region.^{14,29} To establish the change, if any, in the ligand end absorption resulting from complexation to a divalent metal ion, the synthesis and preliminary investigation of complex **2**, the Zn(II) analogue of **1**, was undertaken. Although both complexes **1** and **2** compositionally are identical, powder diffraction studies show that these complexes are not isomorphous. However, it is still possible that the *molecular* structures of **1** and **2** are similar. The special preference of Zn(II) for nitrogen and sulfur donor ligands suggests that complex **2** also contains a N_4S donor set. This issue currently is the subject of a crystallographic study in our laboratories. In view of the large carboxylate rotation observed for **1** (vide supra), it is especially important to characterize the ligand-localized (near UV) transitions of a reference Zn^{II}-mercaptide complex.

Complex **2** appears to be an attractive electronic-spectral reference; its spectra also have been included in Figure 3. Since the Zn(II) analogue as well as free mercaptobenzoate only exhibits end absorption in the UV region, the absorptions of **1** at 360, 418, and ~ 430 nm reasonably may be assigned to $\text{S} \rightarrow \text{Cu(II)}$ LMCT. The existence of a single d vacancy on Cu(II) coupled with the presence of three different lone pairs on the mercaptide sulfur may in principle result in three LMCT absorptions. More specifically, the relatively intense high-energy absorption at 360 nm likely has considerable $\sigma \rightarrow$

Table V. Hydrogen-Bonding Contacts in **1**

donor (D)	hydrogen (H)	acceptor (A)	D-H...A, deg	D...A, Å	H...A, Å	D-H, Å
N	H(N3)	O(1) i ^a	168	2.89(1)	2.01	0.88
O	H2(O3)	O(2) i	168	2.88(2)	1.91	0.98
O	H2(O3)	O(1) i	123	3.02(2)	2.34	0.98
N	H(N2)	O(2) ii	161	3.01(1)	2.19	0.86
N	H(N4)	O(2) ii	155	3.06(1)	2.22	0.90

^a i = x, y, z; ii = -x, -y, -z.

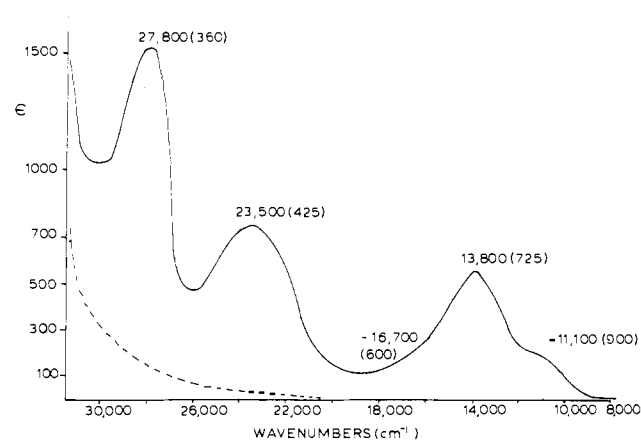


Figure 4. Electronic spectra of **1** (—) and of free mercaptobenzoate (- - -) in 0.01 M methanolic KOH at 25 °C. Peak positions in nanometers are given in parentheses.

σ^* character, and is assigned as $\sigma(\text{S}) \rightarrow \text{Cu(II)}$ LMCT. The red-shifted and weaker absorptions at 418 and 430 nm are assigned to $\pi(\text{S}) \rightarrow \text{Cu(II)}$ LMCT which has become resolved in the relatively low symmetry of **1**.³⁰ This interpretation yields a separation of σ, π LMCT of ~ 4500 cm^{-1} ; the separation of possibly analogous spectral features exhibited by several blue (type 1) copper proteins spans the range 3800–4800 cm^{-1} .³¹ The apparent blue shift of $\text{S} \rightarrow \text{Cu(II)}$ LMCT in **1** relative to that assigned to the blue proteins may result from a number of factors. First, the energy of the copper d vacancy in the proteins will reflect their approximately tetrahedral N_2SS^* ligand donor sets.² The energy of the copper d vacancy in **1** should be higher owing to the stronger ligand field of the trigonal bipyramidal N_4S donor set. The average energy of the ligand field absorptions reported for the proteins³¹ is ~ 5000 cm^{-1} lower than the average energy observed for **1**. Secondly, LMCT absorptions of **1** should be in part blue shifted because the resulting Cu(I) ion is destabilized by the saturated nitrogen macrocyclic ligand. Electrochemically generated Cu^I-tet

complexes are unstable with respect to disproportionation.³² In contrast, the high redox potentials observed for the blue proteins imply that Cu(II) is destabilized with respect to Cu(I). The "hard" ligand donor set of **1** serves to raise the energy of the LMCT excited state and further blue shift such absorptions.

Finally, we note that the polarographically determined half-wave oxidation potential of free 2-mercaptobenzoate at the pH used to prepare **1** (pH ~12) is ~-0.49 V relative to a SCE.³³ Under comparable conditions, other deprotonated alkyl and aryl mercaptides exhibited similar potentials, e.g., reduced glutathione,³⁴ -0.48 V; cysteine,³⁴ -0.58 V; 2-mercaptoethanol,³⁴ -0.54 V; 2-mercaptoethylamine,³⁴ -0.56 V; benzenethiol,³⁵ -0.50 V; 3-mercaptobenzoate,³⁵ -0.50 V. Thus, the potential of 2-mercaptobenzoate is typical of deprotonated aryl and alkyl mercaptides, and, most importantly, is nearly identical with that of the -CH₂SH side chain of reduced glutathione. Neither the surprising stability of **1** nor the relatively high energy of its S → Cu(II) LMCT absorptions can be attributed to atypical redox behavior of the mercaptobenzoate ligand.³⁶

Acknowledgments. This work was supported by the National Institutes of Health (Grant AM-16412 to H.J.S.) and the Rutgers Computing Center. We thank Mr. Mario Nappa and Mr. William Schwindinger for obtaining the ESR and susceptibility data, respectively. We thank Professor David N. Hendrickson for communicating the preliminary results of his ESR studies of complex **1**.

Supplementary Material Available: A list of observed and calculated structure factors (10 pages). Ordering information is given on any current masthead page.

References and Notes

- (1) (a) Rutgers University, New Brunswick; (b) Rutgers University, Newark.
- (2) Recent crystallographic and sequencing studies have shown that an approximately tetrahedral Cu^IN₂(imidazole)S(cysteine)S*(methionine) unit serves as the chromophore for the plastocyanins and azurins. It is clear that Cu^I-S(cysteine) bonding will be common to all of the type 1 chromophores, including the methionine-free protein stellacyanin. See P. M. Colman, H. C. Freeman, J. M. Guss, M. Murata, V. A. Norris, J. A. M. Ramshaw, and M. P. Venkatappa, *Nature (London)*, **272**, 319 (1978), and references cited therein.
- (3) R. D. Bereman, F. T. Wang, J. Najdzionek, and D. M. Braitsch, *J. Am. Chem. Soc.*, **98**, 7266 (1976).
- (4) Y. Sigiura and Y. Hirayama, *J. Am. Chem. Soc.*, **99**, 1521 (1977).
- (5) A. R. Amundsen, J. Whelan, and B. Bosnich, *J. Am. Chem. Soc.*, **99**, 6730 (1977).
- (6) J. S. Thompson, T. J. Marks, and J. A. Ibers, *Proc. Natl. Acad. Sci. U.S.A.*, **74**, 3114 (1977).
- (7) H. J. Schugar, C. C. Ou, J. A. Thich, J. A. Potenza, R. A. Lalancette, and W. Furey, Jr., *J. Am. Chem. Soc.*, **98**, 3047 (1976).
- (8) P. J. M. W. L. Birker and H. C. Freeman, *J. Am. Chem. Soc.*, **99**, 6890 (1977).
- (9) D. Mastropaolo, J. A. Thich, J. A. Potenza, and H. J. Schugar, *J. Am. Chem. Soc.*, **99**, 424 (1977).
- (10) D. K. Cabiness and D. W. Margerum, *J. Am. Chem. Soc.*, **92**, 2151 (1970).
- (11) The Co(II) analogue of **1** and **2** has been obtained in crystalline form and is the subject of current crystallographic and spectroscopic studies: J. L. Hughey IV and H. J. Schugar, unpublished studies.
- (12) A. M. Tait and D. H. Busch, *Inorg. Nucl. Chem. Lett.*, **8**, 491 (1972); W. F. Curtis and R. W. Hay, *Chem. Commun.*, 524 (1966).
- (13) N. F. Curtis, *J. Chem. Soc.*, 2644 (1964).
- (14) G. R. Schoenbaum and M. L. Bender, *J. Am. Chem. Soc.*, **82**, 1900 (1960).
- (15) In addition to local programs for the IBM 360/67 computer, local modifications of the following programs were employed: LPCOR absorption program; Zalkin's FORDAP Fourier program; Johnson's ORTEP II thermal ellipsoid plotting program; Busing, Martin, and Levy's ORFEE error function; and the FLINUS least-squares program obtained from Brookhaven National Laboratories. The analysis of variance was carried out using program NANOVA obtained from Professor I. Bernal: J. S. Ricci, Jr., C. A. Eggers, and I. Bernal, *Inorg. Chim. Acta*, **6**, 97 (1972).
- (16) (a) Scattering factors were obtained from the "International Tables for X-ray Crystallography", Vol. IV, Kynoch Press, Birmingham, England, 1974, pp 71-98; (b) *ibid.*, pp 148-151.
- (17) M. R. Churchill, *Inorg. Chem.*, **12**, 1213 (1973).
- (18) See paragraph at end of paper regarding supplementary material.
- (19) C. C. Ou, V. M. Miskowski, R. A. Lalancette, J. A. Potenza, and H. J. Schugar, *Inorg. Chem.*, **15**, 3157 (1976), and references cited therein.
- (20) R. A. Bauer, W. R. Robinson, and D. W. Margerum, *J. Chem. Soc., Chem. Commun.*, 289 (1973).
- (21) D. M. Duggan, R. G. Jungst, K. R. Mann, G. D. Stucky, and D. N. Hendrickson, *J. Am. Chem. Soc.*, **96**, 3443 (1974).
- (22) P. O. Whimp, M. F. Bailey, and N. F. Curtis, *J. Chem. Soc. A*, 1956 (1970).
- (23) G. Ferguson and G. A. Sim, *Acta Crystallogr.*, **14**, 1262 (1961).
- (24) Y. Okaya, *Acta Crystallogr.*, **22**, 104 (1967).
- (25) The reported magnetic moment includes a diamagnetic correction of -323 × 10⁻⁶ cgs (per Cu) which has been calculated from Pascal's constants.
- (26) M. C. Styka, R. C. Smierciak, E. L. Blinn, R. E. DeSimone, and J. V. Pas-sariello, *Inorg. Chem.*, **17**, 82 (1978).
- (27) Professor David N. Hendrickson, private communication.
- (28) Although the KBr pellets appeared to be clear green glasses, microscopic examination revealed that **1** was present in a dispersed, but not dissolved, state. Solutions of **1** in methanolic KOH follow Beer's law over the concentration range 0.4 × 10⁻³ to 2 × 10⁻³ M; studies at higher concentrations were not possible owing to the limited solubility of **1** in methanol at 25 °C. The marked difference between the ε values of crystalline and dissolved **1** was reproducible. These results imply that solvation of **1** is accompanied by certain changes in the geometry of the Cu(II) coordination sphere which affect the intensity, but not the position, of the absorption bands.
- (29) To observe the spectra of the dianion better, we have extended the spectral study in ref 14 from pH 8 to pH ~12. The pK_a for o-HSC₆H₄CO₂⁻ is 8.88. See R. J. Irving, L. Nelander, and I. Wadsö, *Acta Chem. Scand.*, **18**, 769 (1964).
- (30) We are attempting to prepare a chiral analogue of **1** with optically resolved tet b. A comparison of the optical and MCD spectra may help to differentiate σ and π LMCT.
- (31) Electronic absorptions at ~600 (ε >3000) and ~800 nm (ε 400-1300) have been assigned as σ(S) → Cu(II) LMCT and π(S) → Cu(II) LMCT, respectively. See E. I. Solomon, J. W. Hare, and H. B. Gray, *Proc. Natl. Acad. Sci. U.S.A.*, **73**, 1389 (1976), and references cited therein.
- (32) D. C. Olson and J. Vasilevskis, *Inorg. Chem.*, **10**, 463 (1971).
- (33) S. K. Tiwari and A. Kumar, *J. Prakt. Chem.*, **316**, 934 (1974).
- (34) W. Stricks, J. K. Frischman, and R. G. Mueller, *J. Electrochem. Soc.*, **109**, 518 (1962).
- (35) B. Nygard, *Acta Chem. Scand.*, **20**, 1710 (1966).
- (36) Questions raised by the referees prompted us to make these points explicit.